International Journal of Fluid Machinery and Systems
Vol. 4, No. 1, January-March 2011

DOI: 10.5293/IJFMS.2011.4.1.172
ISSN (Online): 1882-9554

Original Paper (Invited)

Optimization of Vane Diffuser in a Mixed-Flow Pump for High Efficiency Design

Jin-Hyuk Kim[1] and Kwang-Yong Kim[2]

[1]Department of Mechanical Engineering, Graduate School, Inha University
253 Yonghyun-Dong, Incheon, 402-751, Republic of Korea, jinhyuk@inha.edu
[2]Department of Mechanical Engineering, Inha University
253 Yonghyun-Dong, Incheon, 402-751, Republic of Korea, kykim@inha.ac.kr

Abstract

This paper presents an optimization procedure for high-efficiency design of a mixed-flow pump. Optimization techniques based on a weighted-average surrogate model are used to optimize a vane diffuser of a mixed-flow pump. Validation of the numerical results is performed through experimental data for head, power and efficiency. Three-level full factorial design is used to generate nine design points within the design space. Three-dimensional Reynolds-averaged Navier-Stokes equations with the shear stress transport turbulence model are discretized by using finite volume approximation and solved on hexahedral grids to evaluate the efficiency as the objective function. In order to reduce pressure loss in the vane diffuser, two variables defining the straight vane length ratio and the diffusion area ratio are selected as design variables in the present optimization. As the results of the design optimization, the efficiency at the design flow coefficient is improved by 7.05% and the off-design efficiencies are also improved in comparison with the reference design.

Keywords: Mixed-flow pump, Impeller, Vane diffuser, Efficiency, Optimization, Weighted-average surrogate model.

1. Introduction

Mixed-flow pump has an intermediate specific speed between axial-flow and centrifugal pumps. Head and shaft power of a mixed-flow pump are less than those of an axial-flow pump, respectively, and the size and weight of a mixed-flow pump are less than those of a centrifugal pump, respectively. Therefore, the present industrial preference for axial-flow pumps or centrifugal pumps is being rapidly replaced by mixed-flow pumps. Due to this trend, the researches for mixed-flow pumps tend to be increasing gradually.

Goto [1] applied an incompressible version of a Navier-Stokes code to the flow analysis of a mixed-flow pump impeller, and the results were validated in comparison with experimental measurements for the mixed-flow pump impeller at four different tip clearances. Muggli et al. [2] reported mixed-flow pump characteristics from shutoff to maximum flow through computational fluid dynamics (CFD) calculations. CFD analysis of the first-stage rotor and stator in a two-stage mixed-flow pump has been performed by Miner [3]. Miyabe et al. [4] investigated the phenomenon of the diffuser rotating stall in a low specific speed mixed-flow pump through a dynamic particle image velocimetry (DPIV) and CFD simulation.

Especially, efficiency of mixed-flow pumps becomes increasingly important for the applications to industrial pumps. Oh and Kim [5] performed the design optimization of mixed-flow pump impellers using a mean streamline analysis. Zangeneh et al. [6] demonstrated the suppression of meridional secondary flows in a mixed-flow pump impeller through controlling the blade pressure distribution by using an inverse design method. Goto and Zangeneh [7] reported the methodology to design the low specific speed pump diffusers having a good efficiency through an inverse design method and CFD simulation.

On the other hand, Goel et al. [8] developed weighted-average surrogate models and concluded that these weighted-average surrogate models were more reliable prediction methods than the individual surrogates. The weighted-average surrogate models consist of response surface approximation (RSA) model [9], Kriging meta-modeling technique (KRG) [10] and radial basis neural network (RBNN) [11]. Samad and Kim [12] reported on the performances of several surrogate models in optimizing a compressor blade shape, and presented that one of the weighted average surrogate models termed WTA3 by Goel et al. [8] showed reliable performance in this application.

In this work, design optimization using the weighted-average surrogate model coupled with three-dimensional Reynolds-averaged Navier-Stokes (RANS) analysis has been performed for design of a vane diffuser in a mixed-flow pump. Two variables

Accepted for publication December 30, 2010: Paper number O10063S
Corresponding author: Kwang-Yong Kim, Professor, kykim@inha.ac.kr
This paper was presented at 2010 International Conference on Pumps and Fans, October 18-21, 2010, Hangzhou, China

related to the shape of diffuser vane were selected as design variables in the present optimization. The objectives of this work are to improve the entire system performance of the mixed-flow pump by means of the proposed design method and to examine the differences in the flow field between the reference and the optimum shapes to gain understanding of the flow physics associated with the improved efficiency.

2. Specification of the Mixed-Flow Pump

In the present study, three-dimensional RANS analysis has been performed in a mixed-flow pump used for irrigation and drainage. A commercial mixed-flow pump which has been verified for the efficiency and specifications by various experiments [13] was selected to use the highly reliable experimental data. The mixed-flow pump model which consists of an impeller with five blades and a diffuser with six vanes has the specific speed, $Ns=N\cdot Q^{0.5}/H^{0.75}=1099.1$ at the best efficiency point (BEP). The volumetric flow rate and the total head at the design-point of the reference model are 568.15 m^3/min and 8.92 m, respectively. The three-dimensional geometry of the mixed-flow pump with the impeller and the vane diffuser is shown in Fig. 1. And, the detailed design specifications are listed in Table 1.

3. Computational Methods

The flow analysis was performed by solving three-dimensional RANS and energy equations through the commercial code ANSYS-CFX 11.0 [14] based on finite-volume solver. Three-dimensional RANS equations with the shear stress transport turbulence (SST) model were discretized by using finite volume approximations. A high-resolution scheme which is second-order accurate in space was used to solve the convection-diffusion equations. The SST model uses a k-ω model at the near-wall region and a k-ε model in the bulk domain; a blending function ensures a smooth transition between the two models, viz., k-ω and k-ε. The accuracy of the numerical scheme for turbulent flow is highly dependent upon the treatment of the wall shear stress. In the present study, the near-wall grid resolution was adjusted to keep $y+ \leq 2$ for applying low-Reynolds-number version of the SST model and accurate capturing of wall shear stress.

The computational domain for the numerical analysis which consists of a single passage of the mixed-flow pump impeller and the vane diffuser is shown in Fig. 1. The flow field was analyzed by assuming that the flow between two adjacent main blades (& vanes) is periodic about the rotation axis. The total pressure and the designed mass flow rate were set at the inlet and outlet for steady-state simulation, respectively. Water was considered as the working fluid, and the solid surfaces were considered to be hydraulically smooth with no-slip and adiabatic conditions. The stage method was used for the connection between the impeller and the vane diffuser stage. The stage method performs a circumferential averaging of the fluxes through bands on the interface [14].

A structured grid system was constructed in the computational domain, which has O-type grids near the blade surfaces and H/J/C/L-type grids in the other regions. The inlet and outlet blocks were constructed using 30,000 and 70,000 grid points, respectively, while the main impeller and vane diffuser passages were constructed using 250,000 and 250,000 grid points, respectively. The optimum grid system selected by the grid-independency test has 600,000 grid points as reported by previous work [13]. Figure 1 shows a typical example of the grid system used for the numerical analysis of the mixed-flow pump. The near-wall mesh progression was kept as 1.2 with a distance of 0.002 mm for the first node.

The root mean squared (RMS) residual values of the momentum and mass were set to fall below 1.0E-05 and the imbalances of mass and energy were kept below 1.0E-02 as part of the convergence criteria. The physical time-scale was set to $0.1/\omega$, where ω is the angular velocity of the blades. The converged solutions were obtained after approximately 600 iterations. The computations have been performed by a PC with an Intel Pentium IV CPU of a clock speed of 3.0 GHz. The computational time was about 8-9 hours depending upon the geometry considered and the rate of convergence.

Table 1 Design specifications of the mixed-flow pump

Flow coefficient	0.74	Tip clearance (mm)	1.0
Rotational speed (r/min)	238.0	Number of main blade (diffuser vane)	5 (6)
Total head (m)	8.92	Maximum diameter of impeller (mm)	1799.0

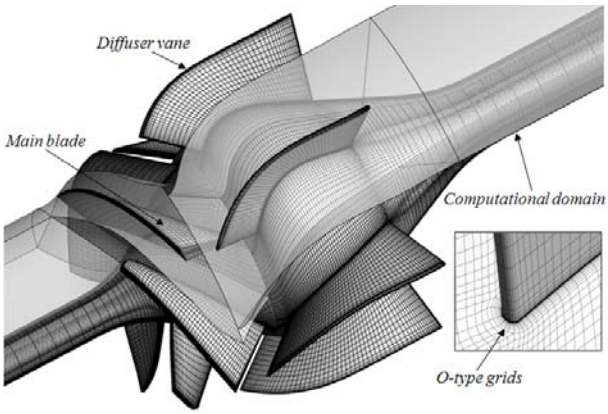

Fig. 1 Three-dimensional geometries and the computational domain of the mixed-flow pump

4. Optimization Techniques

Some pressure losses in the region of the vane diffuser due to undesirable flow structure were observed through the analyses of the internal flow field at the design flow coefficient by previous work [13]. Therefore, in order to reduce the losses for enhancement of pump efficiency, optimal design of the vane diffuser geometry is necessary.

In the present study, the straight vane length ratio (SVLR) and the diffusion area ratio (DAR) were selected as design variables on the basis of the previous work [13], which are defined, respectively, as follows:

$$\text{Straight vane length ratio (SVLR)} = L_2/L_1 \tag{1}$$

$$\text{Diffusion area ratio (DAR)} = A_2/A_1 \tag{2}$$

where, L and A are straight vane length and diffusion area, respectively, as indicated in Fig. 2.

Figure 2 illustrates the SVLR and the DAR section on the vane diffuser. The straight vane is the B-C section ($d\theta=0$) of which diffuser vane angle does not have any changes, and the length ratio is represented as the newly modified straight vane section (B-C′)-to-the straight vane section (B-C) ratio, as shown in Figs. 2(a) and (b). The DAR determined by hub and casing is defined as A_1-to-the area of discharge ratio. Here, A_1 is the smallest flow area located at the place with the largest radius of the hub. And, the hub shape of reference near the discharge area represents the shaft of a mixed-flow pump. Therefore, the DAR is calculated with the only changes of the casing shape of the reference, while hub is fixed by the shaft, as shown in Fig. 2(b). Consequently, the SVLR and the DAR were adopted as design variables in this study.

The purpose of the present optimization is to maximize the efficiency (η), which is defined as:

$$\eta = \frac{\rho g H Q}{P} \tag{3}$$

where, ρ, g, H, Q and P indicate density, acceleration of gravity, total head, volumetric flow rate, and power, respectively. Therefore, through the optimization, the efficiency of the mixed-flow pump is supposed to be maximized with the reduction of pressure loss occurred in the diffuser vane section.

In the present study, the three-level full factorial design of design-of-experiments was used, and one of the weighted-average surrogate models (WTA3 model) proposed by Goel et al. [8] was adopted. This model was called PBA (PRESS-based-averaging) model later by Samad et al. [15]. The predicted response of PBA model is defined based on the PRESS (predicted error sum of squares) as follows:

$$\hat{F}_{wt,avg}(x) = \sum_{i}^{N_{SM}} w_i(x)\hat{F}_i(x) \tag{4}$$

where, N_{SM} is the number of basic surrogate models used to construct the weighted-average model. i^{th} surrogate model at the design point x produces weight $w_i(x)$, and $\hat{F}_i(x)$ is the predicted response by i^{th} surrogate model. The above equation can be written in a simplified form as follows:

$$F_{wt,\,avg} = w_{RSA}F_{RSA} + w_{KRG}F_{KRG} + w_{RBNN}F_{RBNN}$$
$$X_j^l < x_j < X_j^u,\ \text{j= 1,2, 3, …,6.} \tag{5}$$

where, F_{RSA}, F_{KRG} and F_{RBNN} are the responses predicted by the basic surrogates, RSA, KRG, and RBNN, respectively. And, X^l and X^u are the lower and upper bounds on each design variable.

The weights are decided such that the basic surrogate which produces the higher-error has the lower-weight, and thus the lower contribution towards the final weighted-average surrogate, and vice-versa. Global weights are calculated from each basic surrogate using generalized mean square cross-validation (CV) error (GMSE) or PRESS (in RSA terminology). In cross validation, the data is divided into k subsets (k-fold CV) of approximately equal size. A surrogate model is constructed k times, each time leaving out one of the subsets from training, and using the omitted subset to compute the error measure of interest. The generalization error estimate is computed using the k error measures obtained (e.g., average). If k equals the sample size, this approach is called leave-one-out CV (or PRESS).

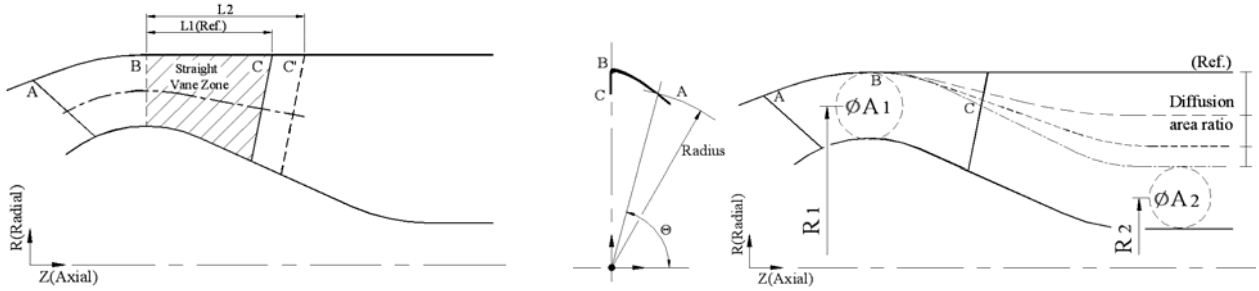

(a) Straight vane length ratio (SVLR) (b) Diffusion area ratio (DAR)

Fig. 2 Definitions of the design variables

After constructing the weighted-average surrogate model, the sequential quadratic programming (SQP) [16] algorithm of optimization is used to search for the optimum point from PBA model. Since the SQP is dependent on initial guess of the optimum point, hence a series of trials have been performed before getting the final optimum point from any surrogate.

5. Results and Discussion

The numerical results of the flow analysis have been validated prior to the design optimization. The shape of the impeller and the diffuser used for this validation was regarded as the reference shape. The numerical results were validated through a comparison with the experimental data in the previous work [13]. Figure 3 shows the validation results in relation to the performance test for the head, efficiency and power. On the whole, the computational heads, efficiencies and powers are in good agreements with the test data for entire flow coefficients. Therefore, it is assured that the numerical analysis of this research has highly ensured validation and reliance.

For the design optimization, it is important to find the feasible and practical design space that is formed with the ranges of the design variables. The ranges of the design variables are presented in Table 2. Each variable is normalized by each reference value. The nine design points were selected by the three-level full factorial design in this design space. Objective function values at the design points were evaluated by RANS analyses, and the results were used to construct individual surrogates as well as to find the PRESS.

The weights were computed, and finally the weighted-average surrogate model was constituted as follows:

$$F_{wt,\,avg} = 0.649F_{RSA} + 0.232F_{KRG} + 0.119F_{RBNN} \tag{6}$$

where, the CV errors were 0.015, 0.047 and 0.094 for the RSA, KRG and RBNN, respectively. Obviously, the highest and lowest CV errors were produced by the RBNN and RSA, respectively. As all the surrogates do not perform well all the time for all the problems, the weighted-average surrogate protects designers from using any poor surrogate. The highest weight is assigned to a surrogate which produces the lowest error to construct the weighted-average surrogate. In the present optimization, the lowest and highest weights were assigned to the RBNN and RSA surrogates as these produces the highest and lowest errors, respectively.

The optimum design variables for the present vane diffuser were found by the weighted-average surrogate model and listed in Table 3. The efficiency at the design flow coefficient for the reference shape is calculated to be 80.79% as shown in Table 3. The SVLR is optimized to be a longer shape, and the DAR is optimized to be a narrower shape. The efficiency of the optimum shape is estimated to be 88.99% by the weighted-average surrogate model, and calculated to be 87.84% by the RANS analysis. The surrogate model gave good prediction with the relative error of 1.3 %. Consequently, the efficiency is improved by 7.05% through the present optimization method in comparison with the reference shape at the design flow coefficient.

Table 2 Ranges of the design variables

Variables	Lower bound	Upper bound
SVLR	0.03	2.56
DAR	0.23	1.00

Table 3 Results of the design optimization

Designs	Design variables		Prediction	CFD calculation	Increment
	SVLR	DAR	Surrogate, %	η, %	η, %
Reference	1.00	1.00	-	80.79	-
Optimum	1.27	0.52	88.99	87.84	7.05

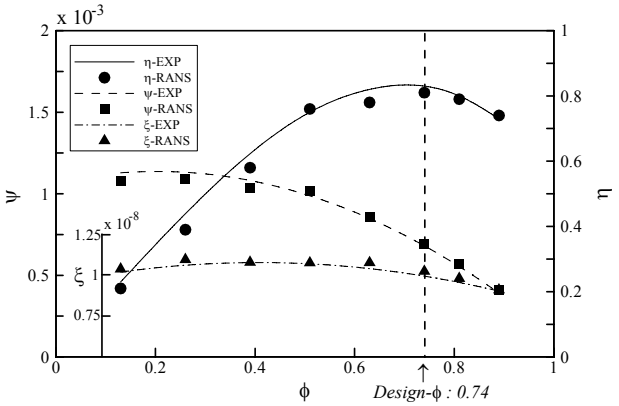

Fig. 3 Validation of the flow analysis [13]

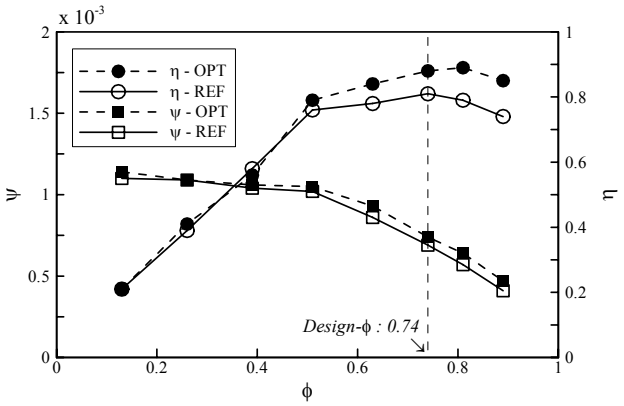

Fig. 4 Performance curves

In order to evaluate the performance at off-design flow coefficients, flow analyses were also performed at several off-design flow coefficients for the reference and the optimum shapes. The results are presented in Fig. 4. Considerable improvement in the efficiency through the optimum shape is observed for the flow coefficient higher than 0.5. It is noted that the optimum shape shows the highest value in the near-runout flow region. And, the reference and optimum shapes have almost similar values of the efficiency in the low flow-rate region. On the other hand, nearly uniform improvement in the head coefficient for the optimum shape is observed throughout the whole flow coefficient range. Thus, the off-design performances are also enhanced by the present optimization.

Figure 5 shows the static pressure distributions on the pressure surface (PS) and suction surface (SS) of the vane diffuser at 20%, 50% and 80% spans. The static pressures on the PS of the reference shape at all spanwise locations commonly decrease rapidly beyond 50% of the streamwise location. Especially, they have the lowest value near the trailing edge (TE). And, the static pressures of the SS are almost constant beyond 50% of the streamwise location. The static pressures on the PS of the optimum shape show the level similar to that of the reference shape, but maintain the level even beyond 50% span unlike the case of the reference shape. And, the static pressures on the SS at all spanwise locations show lower values than those on the SS of the reference shape near the hub, but show higher values near the tip.

The velocity vectors in the optimum and reference shapes at spans of 20%, 50% and 80% are plotted in Fig. 6. A large flow separation is observed on the SS near the TE of the reference diffuser vane across the whole range of the spanwise location. And, the blockage line due to the flow separation in the reference diffuser is shifted to the TE as the tip is approached. It is thought that the entire system efficiency of the reference shape is largely obstructed by the large separation region. However, the flow separation zone is reduced remarkably in the optimum diffuser. And, as the spanwise location is going up, the hydraulic loss becomes smaller, and the flow separation is almost suppressed at 80% span. These show clearly the reason for the enhancement of the efficiency by the optimization.

6. Concluding Remarks

The design optimization of a mixed-flow pump has been performed using PBA weighted-average surrogate model through three-dimensional RANS analyses. In order to reduce some pressure losses in the vane diffuser, the straight vane length ratio, SVLR and diffusion area ratio, DAR were selected as design variables in the optimization. The numerical results were validated in comparison with the experimental data for the heads, powers and efficiencies. The results of the optimization showed that the efficiency at the design flow coefficient is enhanced by 7.05% and the efficiencies at the off-design flow coefficients are also improved significantly in comparison with the reference shape. From the comparison between the reference and

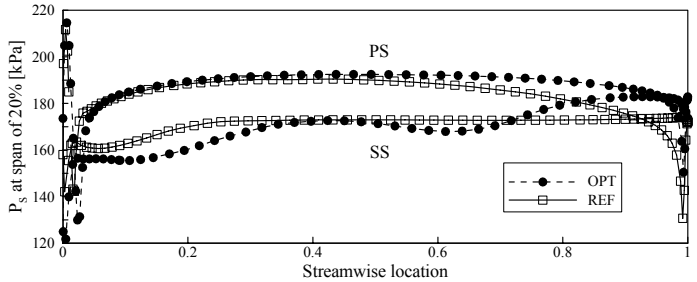

(a) 20% span

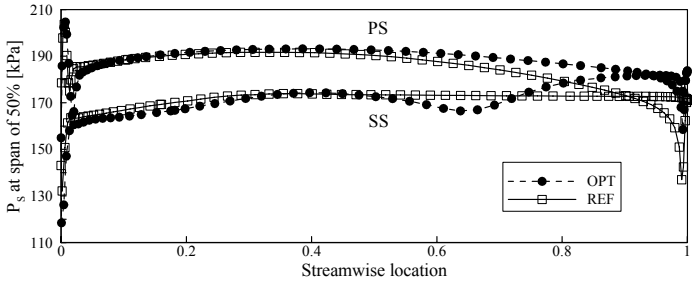

(b) 50% span

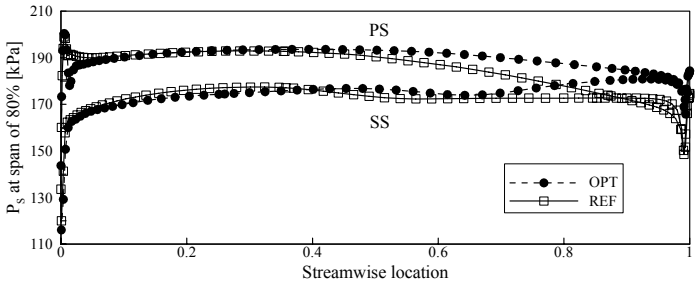

(c) 80% span

Fig. 5 Static pressure distributions on the pressure and suction surfaces of the diffuser vane

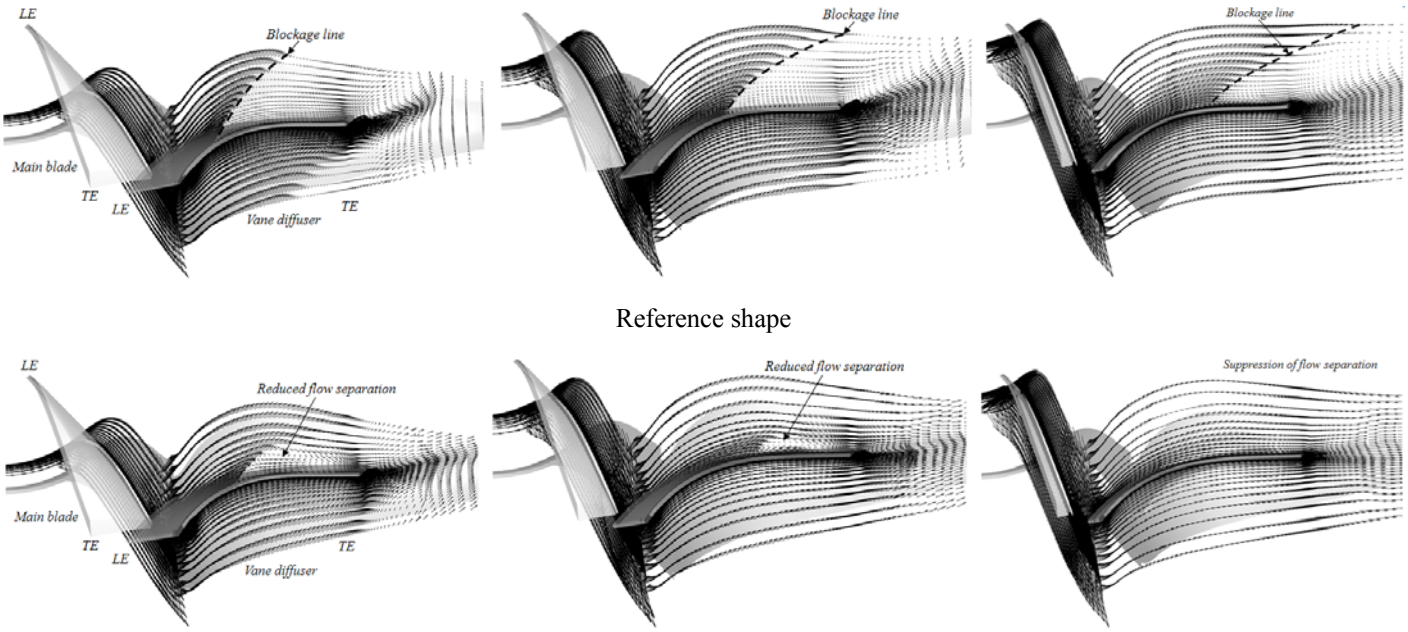

Fig. 6 Velocity vectors in the reference and optimum pumps

optimum shapes, the optimized SVLR and DAR were found to be effective to reduce the flow blockage in the vane diffuser. The entire system performance of a mixed-flow pump was discovered to be improved by reducing pressure loss through the design optimization of the diffuser. However, the optimum design of the vane diffuser can lead a mixed-flow pump out of the design flow coefficient, because the total head can be increased due to the improvement of the efficiency. Therefore, further research needs to be performed concerning the design optimization of the impeller.

Acknowledgments

This research was supported by the Korea Institute of Industrial Technology Evaluation and Planning (ITEP) grant funded by the Ministry of Knowledge Economy (No. 10031771).

Nomenclature

EXP	Experimental data	REF	Reference shape
LE	Leading edge	θ	Diffuser vane angle
OPT	Optimum shape	ξ	Power coefficient, $P/\rho N^3 D^5$
P_S	Static pressure	ϕ	Flow coefficient, Q/ND^3
P_T	Total pressure	ψ	Head coefficient, gH/N^2D^2

References

[1] Goto. A., 1992, "Study of Internal Flows in a Mixed-Flow Pump Impeller at Various Tip Clearances Using Three-Dimensional Viscous Flow Computations," ASME Journal of Turbomachinery, Vol. 114, pp. 373-382.
[2] Muggli, F. A., Holbein, P., and Dupont, P., 2002, "CFD Calculation of a Mixed-Flow Pump Characteristic From Shutoff to Maximum Flow," ASME Journal of Fluids Engineering, Vol. 124, pp. 798-802.
[3] Miner, S. M., 2005, "CFD Analysis of the First-Stage Rotor and Stator in a Two-Stage Mixed Flow Pump," International Journal of Rotating Machinery, Vol. 1, pp. 23-29.
[4] Miyabe, M., Furukawa, A., Maeda, H., Umeki, I., and Jittani. Y., 2009, "A Behavior of the Diffuser Rotating Stall in a Low Specific Speed Mixed-Flow Pump," International Journal of Fluid Machinery and Systems, Vol. 2, No. 1, pp. 31-39.
[5] Oh, H. W., and Kim, K. Y., 2001, "Conceptual design optimization of mixed-flow pump impellers using mean streamline analysis," Proceedings of the Institution of Mechanical Engineers, Part A: Journal of Power and Energy, Vol. 215, No. 1, pp. 133-138.
[6] Zangeneh, M., Goto, A., and Takemura, T., 1996, "Suppression of Secondary Flows in a Mixed-flow pump Impeller by Application of Three-Dimensional Inverse Design Method: Part 1-Design and Numerical Validation," ASME Journal of Turbomachinery, Vol. 118, No. 3, pp. 536-543.
[7] Goto, A., and Zangeneh, M., 2002, "Hydrodynamic Design of Pump Diffuser Using Inverse Design Method and CFD," ASME Journal of Fluids Engineering, Vol. 124, No. 2, pp. 319-328.
[8] Goel, T., Haftka, R. T., Shyy, W., and Queipo, N. V., 2007, "Ensemble of Surrogates," Structural and Multidisciplinary Optimization, Vol. 33, No. 3, pp. 199-216.

[9] Myers, R. H., and Montgomery, D. C., 1995, “Response Surface Methodology-Process and Product Optimization Using Designed Experiments,” John Wiley & Sons, Inc: New York.
[10] Martin, J. D., and Simpson, T. W., 2005, “Use of Kriging Models to Approximate Deterministic Computer Models,” AIAA Journal, Vol. 43, No. 4, pp. 853-863.
[11] Orr, M.J.L., 1996, "Introduction to radial basis neural networks," Center for cognitive science, Edinburgh University, Scotland, UK. http://anc.ed.ac.uk/rbf/.
[12] Samad, A., and Kim, K. Y., 2009, “Application of Surrogate Modeling to Design of A Compressor Blade to Optimize Stacking and Thickness,” International Journal of Fluid Machinery and Systems, Vol. 2, No. 1, pp. 1-12.
[13] Kim, J. H., Ahn, H. J., and Kim, K. Y., 2010, “High-Efficiency Design of a Mixed-Flow Pump,” Science China Technological Sciences, Vol. 53, No. 1, pp. 24-27.
[14] ANSYS CFX-11.0 Solver Theory, 2006, Ansys Inc.
[15] Samad, A., Kim, K.Y., Goel, T., Haftka, R. T. and Shyy, W., 2008, “Multiple Surrogate Modeling for Axial Compressor Blade Shape Optimization,” Journal of Propulsion and Power, Vol. 24, No. 2, pp. 302-310.
[16] MATLAB®, 2004, The Language of Technical Computing, Release 14. The Math Works Inc.